Graphitization Studies of Cured Phenolic Resins by High-Resolution ^{13}C-Cross-Polarization Magic Angle Spinning Solid-State NMR Spectroscopy

B. AMRAM* and F. LAVAL, *Commissariat à l'Energie Atomique, Centre d'Etudes de Vaujours, Service MX, Laboratoire de Résonance Magnétique Nuclèaire, B. P. n° 7, 77181 Country, France*

Synopsis

^{13}C-cross-polarization/magic angle spinning solid-state NMR spectroscopy is used to investigate the graphitization process of a pyrolyzed formophenolic resin. The formation of a 2-dimensional graphitelike lattice, growing with the duration of the laser pyrolysis, is shown. A one-parameter-condensation model is used to estimate, from our dipolar-dephasing NMR experimental data, the quaternary-to-tertiary aromatic fraction, the number of condensed aromatic rings (from 10 to 23 units), and the average cluster diameter (from 9 to 14 Å).

INTRODUCTION

Because of their good ablative properties, phenolic resins are often used as high-temperature polymers.[1,2] The purpose of the present work is to investigate the char formation occurring at very elevated temperatures (> 1000°C) in phenolic resins. The thermal decomposition of those polymeric materials was simulated by a laser pyrolysis. Because they are completely insoluble in all solvents, one of the most useful tools for a quantitative study of their degradation is high-resolution ^{13}C-solid-state NMR spectroscopy. The combined use of cross polarization (CP), high power decoupling, and magic angle spinning (MAS) has enabled high resolution ^{13}C spectra of the solid polymers to be obtained.[3-5]

EXPERIMENTAL

Preparation of Samples

The resol-type materials were prepared by Rhone-Poulenc (France) by condensing phenol and formaldehyde (1 : 2) under basic conditions (amine catalysis). Samples were then heated under vacuum for 24 h at 90°C and 48 h at 170°C. Phenolic resin cylinders (diameter: 13 mm, height: 14 mm) were cut from the same bar. Two of them were kept as reference samples, the others were placed under a CO_2-laser beam (wavelength 10.6 μm) for various times

*Present address: Laboratoire de Physico-Chimie Structurale et Macromoléculaire, ESPCI, 10, rue Vauquelin, 75231 Paris Cedex 05, France.

Journal of Applied Polymer Science, Vol. 37, 1–14 (1989)

CCC 0021-8995/89/010001-14$04.00

(1, 2, 5, and 10 min). The mean energy density was 50 W/cm^2. The portions that could be scraped out after the pyrolysis were removed from the cylinders. Those pyrolyzed portions and the reference samples were then crushed in order to fill the magic-angle rotor in the NMR probe.

Instrumental

^{13}C-^{1}H cross-polarization measurements were made at 22.638 MHz in a static field of 2.1 T with a Bruker CXP 90 spectrometer. The width of the 90° pulse for ^{1}H spin locking (4.5 μs) was determined with benzene. Rotating-frame H_1 fields were 13 and 52 G for ^{1}H and ^{13}C, respectively. The spinning angle was adjusted to the magic angle (54.7°) on a standard test sample of hexamethylbenzene.

Spectra were obtained on samples ($\simeq$ 0.3 g) in a perdeuterated poly(methylmethacrylate) (PMMA-d_x) rotor spinning at 3.3 kHz using an Andrew-type apparatus. For all experiments, repetition rates of 1.5 s, acquisition times of 9–10 ms, and a band width of 16 kHz were used to collect 10,000 FID/spectrum.

Two series of spectra were obtained for each sample, normal CP/MAS experiments with variable contact time T_{CP} (0.25–10 ms) in order to obtain the aromatic fraction f_a and dipolar-dephasing (DD) experiments with a contact time of 2 ms and a variable delay T_{DD} (0.25–100 μs) in order to obtain the quaternary-to-tertiary aromatic fraction $f_{Q/T}$. Chemical shift scales were calibrated with the rotor's peaks: carbonyl absorption (178 ppm) or quaternary carbon absorption (45 ppm) of PMMA-d_x. The chemical shifts are related to the ^{13}C of tetramethylsilane (TMS). Rotation bands, although they were very small, have been accounted in the integration of the aromatic peaks.

RESULTS AND DISCUSSION

Thermal degradation studies on phenol–formaldehyde resins have been carried out by Conley and co-workers[6–9] using infrared spectroscopy, vapor-phase chromatographic methods as well as thermogravimetric and X-ray analyses. At temperatures as high as 1000°C, it was found that the primary degradation route of phenolic resins is oxidation through a quinone-type intermediate. It was also possible to extend the oxidation mechanism to include the formation of a graphite-like char. This extension was postulated on the simultaneous formation of the char and carbon monoxide.

Ouchi and Honda[10] analyzed, by their mass spectra, gases produced by thermal cracking of phenol–formaldehyde resins. They explained that, from about 700 to about 1400°C, a condensed aromatic structure and a 3-dimensional network among the condensed aromatic rings are produced. From about 1400 to about 2000°C, the residual carbons behave like graphite and have a negative temperature dependence of diamagnetic susceptibility; they have large condensed aromatic rings and a 2-dimensional graphitelike lattice.

High resolution ^{13}C CP/MAS solid-state NMR studies of the thermal decomposition of phenolic resins have been extremely limited. An investigation has been made by Fyfe and co-workers[11,12] at temperatures as high as 400°C. They have pointed out the formation, by an oxidative mechanism, of an almost completely aromatic structure with few methylene linking groups.

Our purpose, in this work, is to determine quantitatively, by high resolution ^{13}C-CP/MAS solid-state NMR, the structure of the char obtained from a cured phenolic resin obtained from a cured phenolic resin heated by a laser beam up to about 1500°C.

The ^{13}C-^{1}H CP/MAS technique is based on the transfer of magnetization from the proton system to that of carbon-13 under appropriate conditions.[4] This transfer is governed, for a given carbon, by two important parameters which are the cross-polarization time T_{CH} of the observed carbon atom and the spin–lattice relaxation time $T_{1\rho H}$ of the protons in the rotating frame. In general T_{CH} is much shorter than $T_{1\rho H}$ and the evolution of the ^{13}C-NMR integrated intensity M with the contact time T_{CP} between the two systems is dominated by T_{CH} at short T_{CP} and by $T_{1\rho H}$ at long T_{CP}[13]:

$$M = M_0[1 - \exp(-T_{CP}/T_{CH})]\exp(-T_{CP}/T_{1\rho H}) \quad (1)$$

Thus, qualitatively, at short T_{CP} (≤ 10 μs) only the protonated CH and CH_2 are magnetized and appear on the spectrum (because they rotate, the CH_3 are slower magnetized). For a quantitative measurement, the tail of the variable contact time curve was fit to a single decaying exponential in the region where $T_{CP} \gg T_{CH}$. By extrapolating this monoexponential (monologarithmic scale) to $T_{CP} = 0$, M_0, proportional to the number of carbons, was obtained. The aromatic fraction f_a was calculated by

$$f_a = M_{0Ar}/(M_{0Ar} + M_{0Al}) \quad (2)$$

where M_{0Ar} and M_{0Al} are respectively the aromatic and aliphatic extrapolated intensities. The time constant $T_{1\rho H}$ of the single decaying exponential was also measured.

The dipolar-dephasing experiment is similar to a conventional cross-polarization experiment except for the introduction of a delay T_{DD} between the contact time and the acquisition.[14] During this period, carbons relax differently according to their environments. The aromatic peaks due to protonated (CH) and quaternary carbons were studied by this method. The methynes relax rapidly whereas quaternary carbons relax slower. Thus, qualitatively, at long T_{DD} (≥ 60 μs) only the latter appear in the spectrum and the evolution of the ^{13}C-NMR integrated intensity M_Q is given by[13]

$$M_Q = M_{0Q}\exp(-T_{DD}/T_2^*) \quad (3)$$

where T_2^* is a characteristic time decay. For a quantitative measurement M_{0Q}, proportional to the number of nonprotonated carbons, has to be determined by extrapolating to $T_{DD} = 0$ the linearly decreasing intensity (monologarithmic scale) at long T_{DD}. Using the relation

$$M_0 = M_{0Q} + M_{0T} \quad (4)$$

where M_0 is the total aromatic integrated intensity with no dipolar-dephasing ($T_{DD} = 0.25$ μs $\simeq 0$) and M_{0T} the tertiary aromatic integrated intensity, the

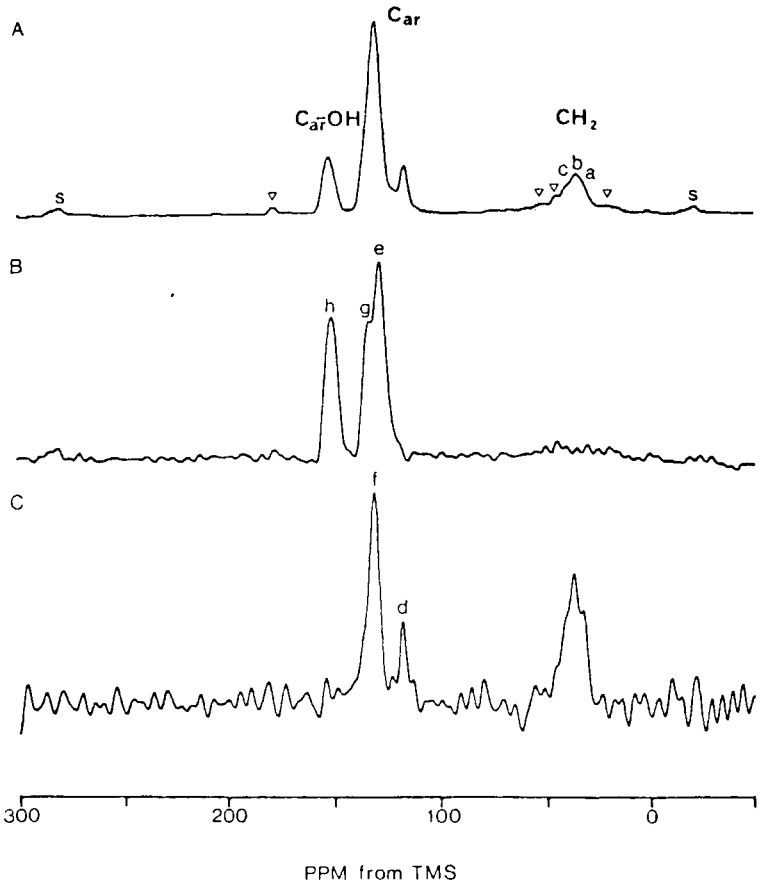

Fig. 1. Solid-state CP/MAS ^{13}C-NMR spectra of the cured unpyrolyzed phenolic resin obtained under the following experimental conditions: (A) normal cross-polarization spectrum: 2μs contact time; (B) dipolar-dephasing spectrum: conditions as in (A) except the introduction of a delay of 80 μs before acquisition; (C) short contact time cross-polyarization spectrum: 5-μs contact time, other conditions as in (A). The small peaks marked s denote spinning side bans, those marked ▽ are for the PMMA-d_x rotor. The sample's peaks are reference according to their designations in Table I.

quaternary-to-tertiary aromatic ratio is given by[15]

$$f_{Q/T} = M_{0Q}/(M_0 - M_{0Q}) \tag{5}$$

Characterization of the Original Unpyrolyzed Cured Phenolic Resin

The spectra obtained for the reference unpyrolyzed sample are shown in Figure 1. Figure 1(A) shows the normal cross-polarization spectrum, Figure 1(B) the spectrum at long T_{DD} of only those carbons with no proton attached, and Figure 1(C) the spectrum at short T_{CP} of only protonated carbons. The aliphatic peak is due to methylene bridges —CH_2—, the aromatic peaks are for carbons C_{ar}—OH bearing the hydroxyl group (152 ppm) and for the remaining ring carbons C_{ar} (130 and 116 ppm).

TABLE I
^{13}C-NMR Structure/Shift[a] Relationships for the Reference Unpyrolyzed Resol

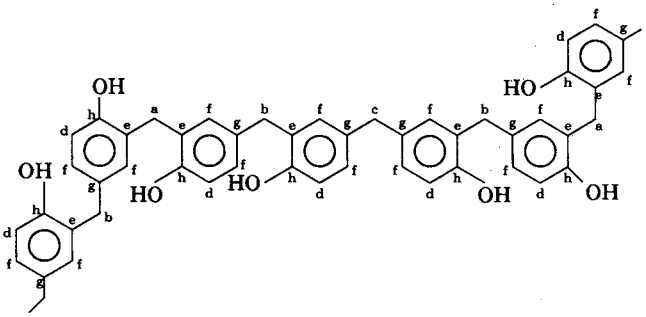

$\delta_{obs\ sol}$ (ppm[b])	Carbon	Type of carbon[c]	$\delta_{calcd.}$ (ppm[d])	$\delta_{liq.}$ (ppm[e])
31	a	Ortho–ortho methylene bridge		31
35	b	Ortho–para methylene bridge		35
39	c	Para–para methylene bridge		41
116	d	Unsubstituted ortho aromatic	116	116
129	e	CH_2-substituted ortho aromatic	128	127–130
131	f	Unsubstituted meta aromatic	127–130	
134	g	CH_2-substituted para aromatic	132	133
152	h	OH-substituted aromatic	155	155

[a]All chemical shifts are relative to tetramethylsilane.
[b]Shifts observed in the solid-state by ^{13}C CP/MAS NMR.
[c]Ortho, meta, and para designations are relative to the OH-substituted carbon.
[d]Shifts calculated with empirical parameters for substituted benzenes.[17]
[e]Solution-state chemical shifts from the literature.[16]

Peaks were assigned on the basis of comparison with solution-state ^{13}C-NMR data in the literature[16] and with shifts calculated with empirical parameters for the calculation of chemical shifts in substituted benzenes.[17] The absence of unsubstituted para aromatic carbons (δ_{calc} = 119 ppm, δ_{sol} = 120 ppm) was noted. A summary of the structure/shift relationships is given in Table I.

The aromatic fraction f_a and the quaternary-to-tertiary aromatic ratio $f_{Q/T}$ were respectively found to be 0.85 and 0.82. These values then imply that there is one methylene bridge and two methylene-bearing aromatic carbons for one phenolic ring (theoretical values: f_a = 0.86, $F_{Q/T}$ = 1.00). Thus it can be concluded that the reference unpyrolyzed resin has a linear structure (see structure in Table I).

Influence of the Time of Pyrolysis on the Aromatic Fraction f_a

The effect of pyrolysis on the phenolic resin is shown in Figure 2. Figure 2(A) shows the reference unpyrolyzed spectrum, and Figure 2(B) shows the significant modifications made by the pyrolysis. The spectrum becomes mainly aromatic and is characteristic of a coal char.[18] The aromatic region is transformed into a broad resonance at 110–140 ppm with residual hydroxyl-bearing carbon peak centered at 150 ppm. The aliphatic resonances gave a substantial

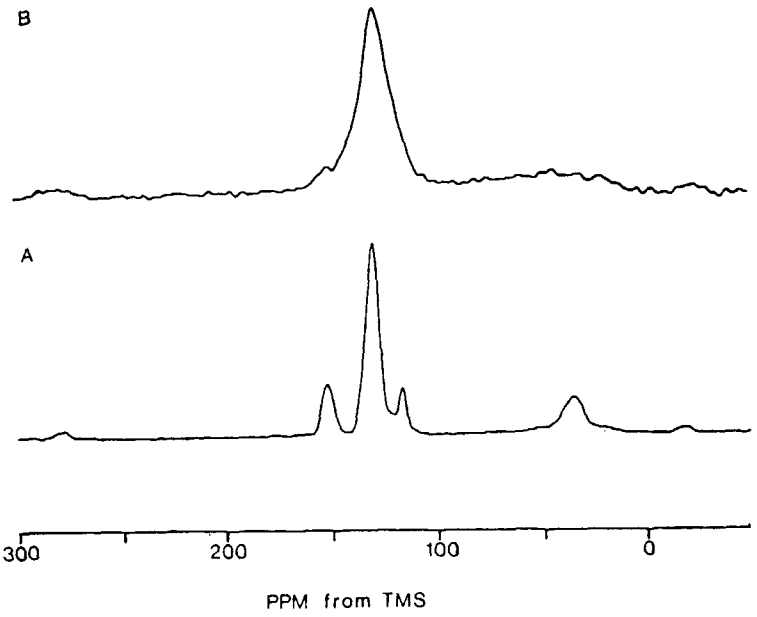

Fig. 2. Effect of the pyrolysis on the phenolic resin: (A) 0.75-ms cross-polarization spectrum of the unpyrolyzed phenolic resin; (B) 0.75-ms cross-polarization spectrum of a phenolic resin taken from the same bar and pyrolyzed for 10 min under a laser beam. The experimental conditions are the same as in (A).

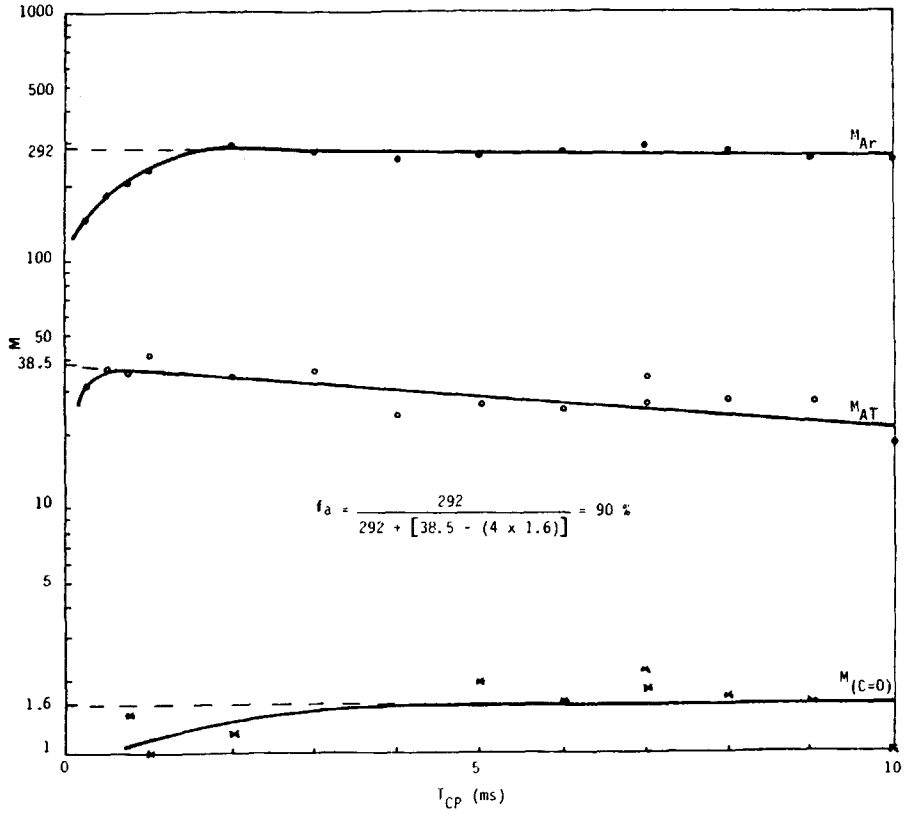

Fig. 3. Integrated intensities of the aromatic region [M_{Ar} (●)], the aliphatic region [M_{Al} (○)] and the carbonyl peak from the PMMA rotor [$M_{(C=O)}$ (*)] vs. contact time T_{CP} (monologarithmic scale). This example is taken for the 5-min pyrolyzed resol.

TABLE II
Aromatic Fraction f_a in the Different Pyrolyzed Phenolic Resins

t_p, duration of the pyrolysis (min)	f_a, aromatic fraction[a]
0[b]	0.85
1	0.90
2	0.90
5	0.90
10	0.89

[a] The aromatic fraction is the ratio of the number of aromatic carbons on the total number of carbons.
[b] I.e., the reference unpyrolyzed resol.

increase in linewidth; their integration therefore took into account a wider range of the spectrum (from 0 to 90 ppm).

In Figure 3 the integrated aliphatic and aromatic intensities are plotted against the contact time T_{CP}. For all samples, a maximum value is reached at 1–2 ms followed by a slight decrease characterized by $T_{1\rho H}$. Linear least-square fitting for $T_{CP} \geq 2$ ms and extrapolation to $T_{CP} = 0$ allowed to reach the aromatic fraction f_a for each pyrolyzed sample (Table II). It must be noted that, before calculating f_a, a correction was made on M_{0Al} because of the presence of the rotor's peaks in the aliphatic region. This rotor's contribution was determined experimentally to be four times the extrapolated magnetiza-

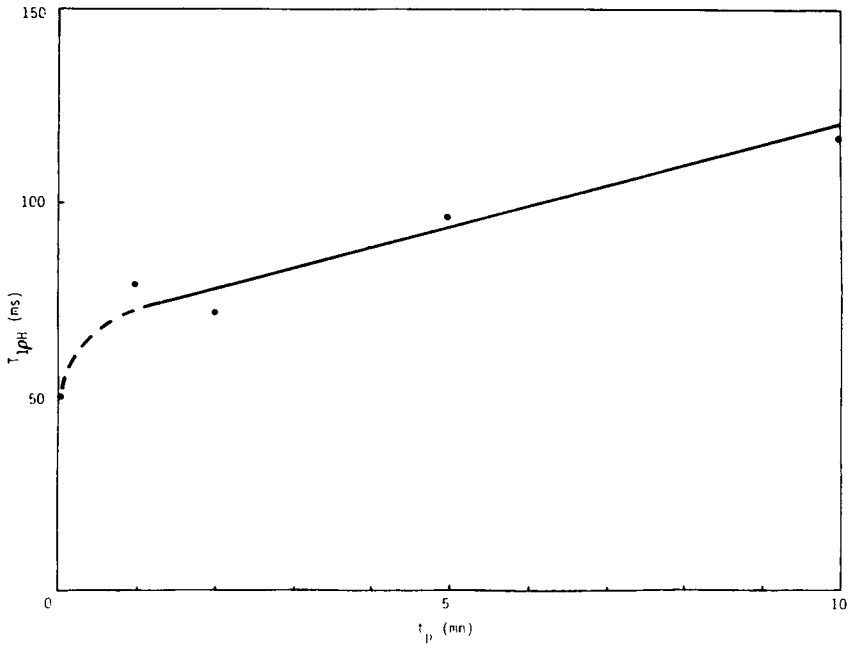

Fig. 4. Evolution of the spin-lattice relaxation time $T_{1\rho H}$ of the aromatic protons in the rotating frame vs. t_p, duration of the pyrolysis of the resol-type sample.

tion $M_{0(C=O)}$ of the PMMA–carbonyl at 178 ppm (because this contribution corresponds to four nuclei: CH_3, C_q, $O-CH_3$, and CH_2) and was subtracted from M_{0Al}. The enhancement of f_a from the reference sample (0.85) to the pyrolyzed ones (0.90) is pointed out, but f_a remains constant with the time of pyrolysis (from 1 to 10 min). However, $T_{1\rho H}$ increases significantly with the time t_p of pyrolysis. There is an approximately linear relationship between $T_{1\rho H}$ and t_p from $t_p = 1$ to 10 min (Fig. 4). This increase pointed out for pyrolyzed phenolic resins may be explained by an increase in structural regularity because of the formation of a graphitic lattice during the pyrolysis.

Influence of the Time of Pyrolysis on the Quaternary-to-Tertiary Aromatic Ratio $f_{Q/T}$

Figure 5 shows the integrated intensities versus dipolar-dephasing time T_{DD} for the aromatic region (90–160 ppm) of the pyrolyzed samples. Linear least-square fitting for $T_{DD} \geq 60$ μs and extrapolation to $T_{DD} = 0$ yielded the quaternary-to-tertiary aromatic ratio $f_{Q/T}$. The results obtained for the series of four samples that are reported in Figure 6 show that $f_{Q/T}$ increases with the time of pyrolysis (i.e., with the thermic energy given to the resin). The value of $f_{Q/T}$ obtained for the unpyrolyzed sample is also plotted in Figure 6 for comparison. Thus, in the aromatic rings, there are more quaternary carbons during the pyrolysis.

Evaluation of the Aromatic Ring Condensation

The NMR-measured aromatic fraction f_a being 0.90, the assumption was made that all ^{13}C of the pyrolyzed resins, characterized as high rank coals, are either tertiary or quaternary aromatic carbons ($f_a = 1.0$). A model of pericondensed 2-dimensional sheet of aromatic rings was formulated by Murphy and co-workers[19] to study the structure of an anthracite coal. It was a two-parameter model: the length and the width of the sheet in units of rings. Consequently, they needed to introduce two experimental data in their equations: $f_{Q/T}$, determined by dipolar-dephasing CP/MAS ^{13}C-NMR and $\overline{D}$, the average cluster diameter estimated from previously reported X-ray and electron microscopy data.

Our purpose was to determine the number of pericondensed aromatic rings and the average cluster diameter without any assumption concerning this diameter. The methodology was to build a one-parameter model consisting of a 2-dimensional cluster growing isotropically during the pyrolysis (Fig. 7). It must be noted that the graphitization is only characterized by its 2-dimensional growth; the stacking of the layers is not estimated by this method.

The aromatic ring cluster is characterized by only one parameter: n, the number of condensed ring-crowns with $n = 1$ for a single benzene ring. The average diameter $\overline{D}$ and the number r of condensed rings can thus be written as functions of n (see Fig. 8):

$$\overline{D} = (2n - 1)d \tag{6}$$

where d is of 2.42 Å, the distance between two parallel bonds in a single ring, when the carbon–carbon bond distance and the angle $\widehat{CCC}$ are respectively

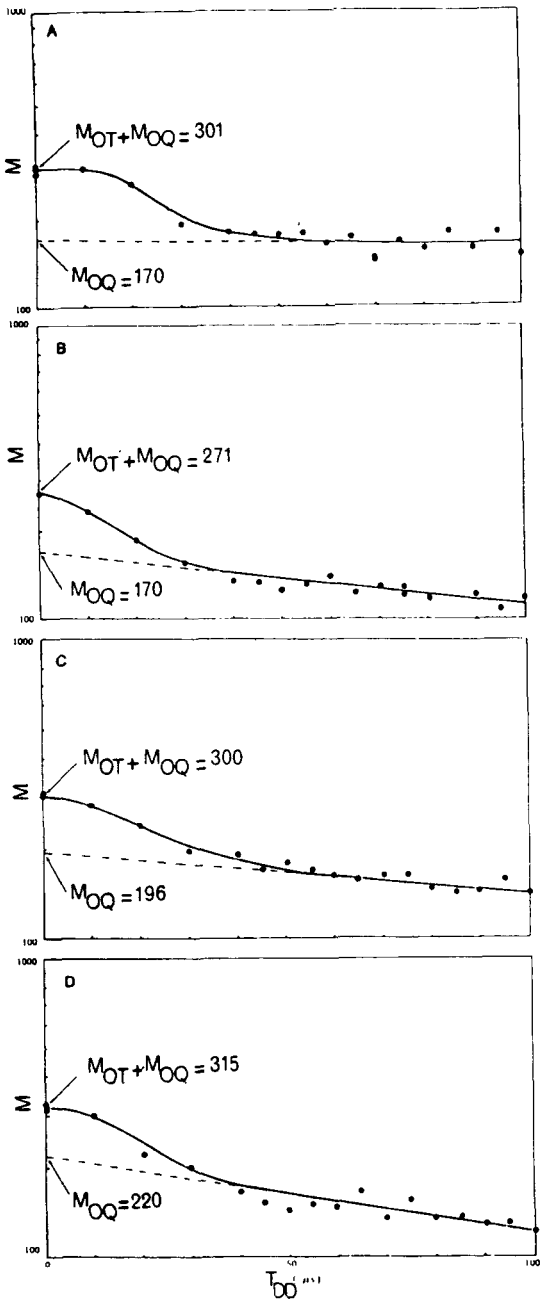

Fig. 5. Aromatic integrated intensity vs. dipolar-dephasing time T_{DD} (monologarithmic scale). The samples are obtained from the same phenolic resin by pyrolysis for different times: (A) 1 min; (B) 2 min; (C) 5 min; (D) 10 min.

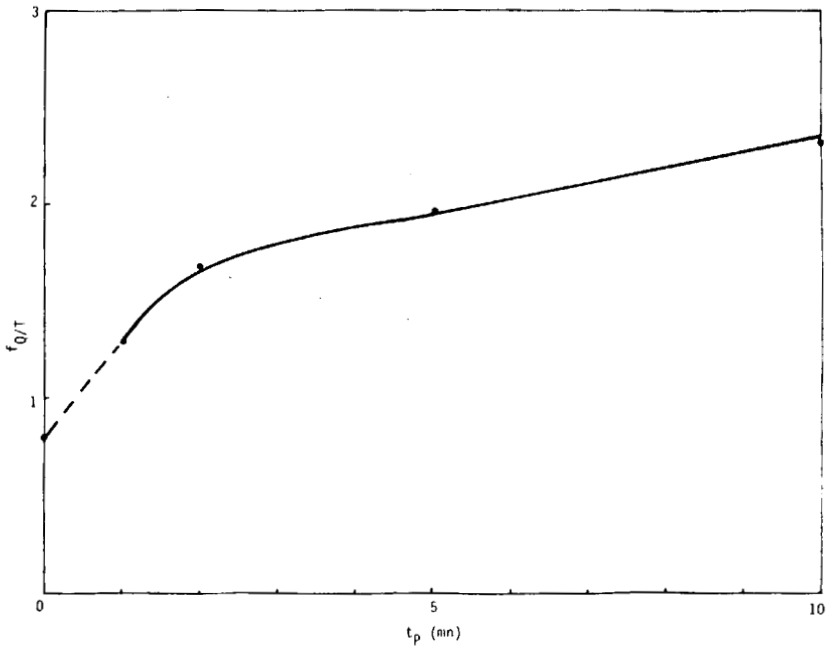

Fig. 6. Evolution of the quaternary-to-tertiary aromatic ration $f_{Q/T}$ vs. t_p, duration of the pyrolysis of the resol-type sample.

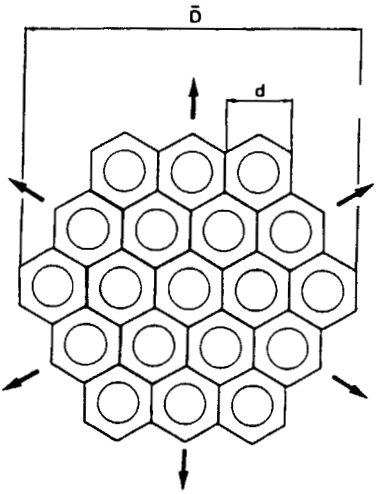

Fig. 7. One-parameter model for aromatic ring condensation. $\bar{D}$ represents the average diameter of the cluster; d is the pseudodiameter of a single ring.

assumed to be 1.40 Å and 120°, and $r = 1 + 6 + 2 \times 6 + 3 \times 6 + \cdots + (n - 1) \times 6$ i.e.,

$$r = 1 + 3n(n - 1) \tag{7}$$

The quaternary-to-tertiary aromatic ratio can also be written as a function

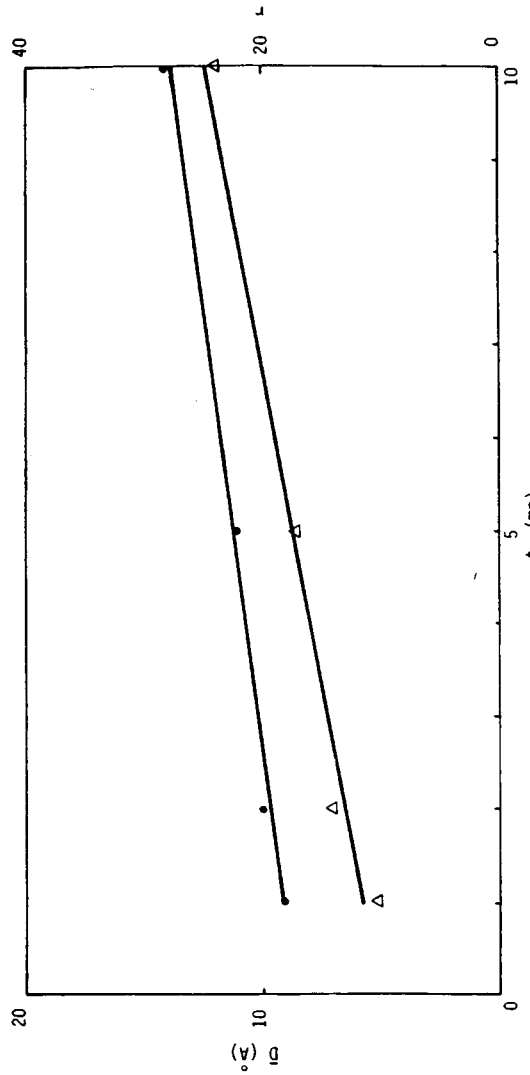

Fig. 8. Evolutions of the average cluster diameter $\bar{D}$ (●) and of the number r (△) of aromatic ring per cluster versus t_p, duration of the pyrolysis of the resol-type sample.

of n:

$$f_{Q/T} = n - 1 \tag{8}$$

From (6)–(8), $\overline{D}$ and r can be written in as functions of $f_{Q/T}$:

$$\overline{D} = (2f_{Q/T} + 1)d \tag{9}$$

$$r = 1 + 3f_{Q/T}(f_{Q/T} + 1) \tag{10}$$

Thus, the determination of $f_{Q/T}$ can yield directly the characteristics (diameter and number of rings) of the average cluster. Figure 8 shows the quasilinear increases of $\overline{D}$ and r with the time of pyrolysis. The average cluster diameter was found to vary from 9 to 14 Å and the number of condensed rings from 10 to 23 units.

In order to estimate the graphitic character of the char, the ring-condensation index f_{RCI} of Van Krevelen[20] was calculated ($f_{RCI} = 0$ for benzene and 1 for graphite):

$$f_{RCI} = 2(r - 1)/N_C \tag{11}$$

N_C being the number of carbon atoms. Using

$$N_C = 6n^2 \tag{12}$$

and eq. (7), f_{RCI} can be written as

$$f_{RCI} = (n - 1)/n \tag{13}$$

or

$$f_{RCI} = f_{Q/T}/(1 + f_{Q/T}) \tag{14}$$

The variations of f_{RCI} with the time of pyrolysis have been plotted in Figure 9. The ring condensation index increases quasi linearly from 0.5 to 0.7 and is thus characteristic of a rather important graphitic condensation increasing with the thermic energy given to the resin. A reaction scheme for the

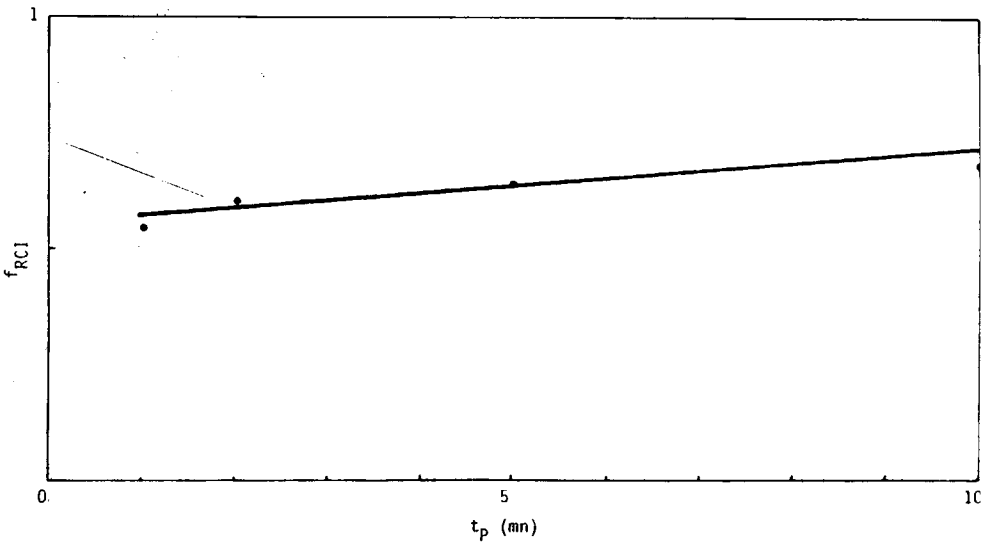

Fig. 9. Evolution of the ring condensation index f_{RCI} vs. t_p, duration of the pyrolysis of the resol-type sample ($f_{RCI} = 0$ for benzene; $f_{RCI} = 1$ for infinite graphite).

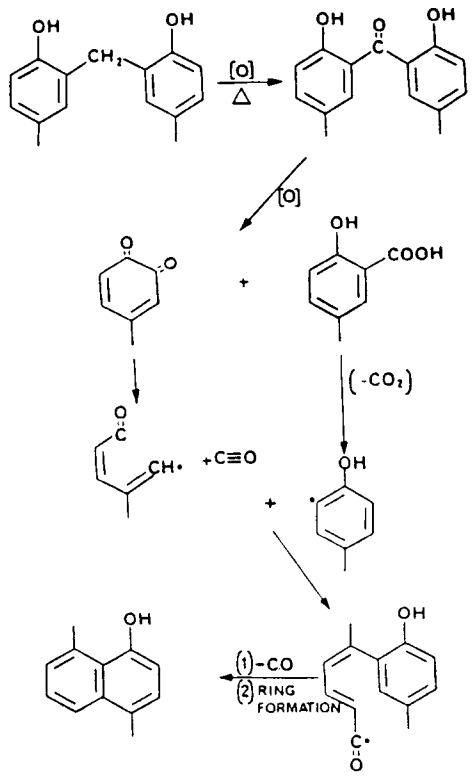

Fig. 10. Reaction scheme postulated by Conley and co-workers[9] for the ring-condensation process in a dihydroxy-diphenylmethane unit during the thermooxidative degreadation of a phenolic resin.

formation of a condensed aromatic ring structure from a phenolic resin has been postulated by Conley and co-workers[9] and is given in Figure 10.

Comparison with Other Data

The quantitative studies on aromatic ring clusters found in the literature have only been made on coal chars but not on pyrolyzed resins. Thus, the comparison with high-rank coals has to be made carefully.

X-ray scattering on an anthracite coal let Hirsch[21] estimate to be about 30 the number of condensed rings and to be about 16 Å the average cluster diameter in a high rank coal (95 wt % C). Using high resolution electron microscopy, Oberlin and Terriere,[22] studying anthracites, gave $\bar{D}$ smaller than 10 Å, i.e., an area less than 10 aromatic rings. Another attempt to illustrate the chemical structure of coals is that of Dryden.[23] Using infrared and X-ray methods, he reported that high rank coals may contain 10–20 fused rings. Assuming that our pyrolyzed resols are high rank coals (elemental analysis gave 94–95 wt % C), our results are of the same magnitude as those previously reported data.

CONCLUSIONS

Using ^{13}C-CP/MAS solid-state NMR spectroscopy and especially dipolar-dephasing experiments, we showed that the very high temperature degrada-

tion of a resol-type phenolic resin leads to the formation of a 2-dimensional graphitelike lattice.

This graphitic character has been estimated quantitatively by determining the number of condensed-aromatic rings in the average molecule and the average diameter of the cluster without help for any other method or previously reported data.

The graphitization was shown to increase with the duration of the laser-pyrolysis. A one-parameter-condensation model led us to estimate the number of condensed rings between 10 (for a 3000 J pyrolysis) and 23 (for a 30,000 J pyrolysis) and the average cluster diameter between 9 Å (for a 3000 J pyrolysis) and 14 Å (for a 30,000 J pyrolysis).

The authors gratefully acknowledge helpful discussions with Professor L. Monnerie and Dr. F. Lauprêtre of the Laboratoire de Physico-Chimie Structurale et Macromoléculaire of the Ecole Supèrieure de Physique et Chimie Industrielles de la Ville de Paris and thank G. Richoux of the Centre d'Etudes Scientifiques et Techniques d'Aquitaine for supplying the reference and pyrolyzed phenolic resins.

References

1. D. L. Schmidt, in *Ablative Plastics*, G. F. D'Alelio and J. A. Parker, Eds., Dekker, New York, 1971.
2. C. L. Segal, *High Temperature Polymers*, Dekker, New York, 1967.
3. D. L. VanderHart, W. L. Earl, and A. N. Garroway, *J. Magn. Reson.*, **44**, 361 (1981).
4. C. S. Yannoni, *Acc. Chem. Res.*, **15**, 201 (1982).
5. D. J. O'Donnell, *Am. Chem. Soc.*, **247**, 21 (1984).
6. R. T. Conley and J. F. Bieron, *J. Appl. Polym. Sci.*, **7**, 103 (1963).
7. W. M. Jackson and R. T. Conley, *J. Appl. Polym. Sci.*, **8**, 2163 (1964).
8. R. T. Conley, *J. Appl. Polym. Sci.*, **9**, 1117 (1965).
9. H. W. Lochte, E. L. Strauss, and R. T. Conley, *J. Appl. Polym. Sci.*, **9**, 2799 (1965).
10. K. Ouchi and H. Honda, *Fuel*, **38**, 429 (1959).
11. C. A. Fyfe, M. S. McKinnon, A. Rudin, and W. J. Tchir, *J. Polym. Sci., Polym. Lett. Ed.*, **21**, 249 (1983).
12. C. A. Fyfe, M. S. McKinnon, A. Rudin, and W. J. Tchir, *Macromolecules*, **16**, 1216 (1983).
13. J. M. Dereppe, *Proceedings of the VIIIth Groupe d'Etudes de Résonance Magnétique*, La Grande Motte, France, 1984, p. 146.
14. S. J. Opella and M. H. Frey, *J. Am. Chem. Soc.*, **101**, 5854 (1979).
15. L. B. Alemany, D. M. Grant, R. J. Pugmire, and L. M. Stock, *Fuel*, **63**, 513 (1984).
16. A. J. J. De Breet, W. Dankelman, W. G. B. Huysmans, and J. de Wit, *Angew. Makromol. Chem.*, **62**, 7 (1977).
17. F. W. Wehrli and T. Wirthlin, *Interpretation of Carbon-13 NMR Spectra*, Heyden, London, 1976, p. 47.
18. M. I. M. Chou, D. R. Dickerson, D. R. McKay, and J. S. Frye, *Liq. Fuels Technol.*, **2** (4), 375 (1984).
19. P. DuBois Murphy, T. J. Cassady, and B. C. Gerstein, *Fuel*, **61**, 1233 (1982).
20. D. W. Van Krevelen, *Coal*, Elsevier, Amsterdam 1961.
21. P. B. Hirsch, *Proc. Roy. Soc. Lond.*, **226A**, 143 (1954).
22. A. Oberlin and G. Terriere, *Carbon*, **13**, 367 (1975).
23. I. G. C. Dryden, *J. Inst. Fuel*, **30**, 193 (1957).

Received August 4, 1986
Accepted November 25, 1987